45. C. Hayashi, K. Nakazawa, Y. Nakagawa, in *Protostars and Planets II*, D. C. Black and M. S. Matthews, Eds. (Univ. of Arizona Press, Tucson, 1985), pp. 1100–1154.
46. E. R. D. Scott, D. J. Barber, C. M. Alexander, R. Hutchison, J. A. Peck, in (*1*), pp. 718–745; B. Donn, *Astron. Astrophys.* **235**, 441 (1990).
47. H. Palme, in (*12*), p. 30.
48. J. W. Larimer and J. T. Wasson, in (*1*), pp. 394–435.
49. H. Palme and W. V. Boynton, in (*3*), pp. 979–1004.
50. I. D. Hutcheon, G. R. Huss, G. J. Wasserburg, *Lunar Planet. Sci.* **XXV**, 587 (1994); I. D. Hutcheon and R. H. Jones, *ibid.* **XXVI**, 647 (1995); G. J. MacPherson *et al.*, *Meteoritics* **30**, 365 (1995).
51. T. Lee, D. A. Papanastassiou, G. J. Wasserburg, *Geophys. Res. Lett.* **3**, 109 (1976); *Astrophys. J.* **211**, L107 (1977).
52. T. Lee, *Astrophys. J.* **224**, 217 (1978); D. D. Clayton and L. Jin, *ibid.* **451**, L87 (1995).
53. N. Sugiura and D. W. Strangeway, in (*1*), pp. 595–615.
54. A. H. Joy, *Astrophys. J.* **102**, 168 (1945); J. G. Bellingham and G. S. Rossano, *Astron. J.* **85**, 555 (1980); J. A. Graham, *Publ. Astron. Soc. Pac.* **104**, 479 (1989); N. L. Eaton and W. Herbst, *Astron. J.* **110**, 2369 (1995).
55. J. T. Armstrong, D. J. Hutter, K. J. Johnston, D. Mozurkewich, *Phys. Today* **48**, 42 (May 1995).
56. R. N. Clayton, T. K. Mayeda, C. A. Molini-Velsko, in (*45*), pp. 755–771.

31 July 1995; accepted 3 January 1996

A Permease-Oxidase Complex Involved in High-Affinity Iron Uptake in Yeast

Robert Stearman, Daniel S. Yuan, Yuko Yamaguchi-Iwai, Richard D. Klausner, Andrew Dancis*

Iron must cross biological membranes to reach essential intracellular enzymes. Two proteins in the plasma membrane of yeast—a multicopper oxidase, encoded by the *FET3* gene, and a permease, encoded by the *FTR1* gene—were shown to mediate high-affinity iron uptake. *FET3* expression was required for FTR1 protein to be transported to the plasma membrane. *FTR1* expression was required for apo-FET3 protein to be loaded with copper and thus acquire oxidase activity. FTR1 protein also played a direct role in iron transport. Mutations in a conserved sequence motif of FTR1 specifically blocked iron transport.

Cells require iron for a wide array of metabolic functions (*1*, *2*), and yet iron can be toxic when present in excess (*3*). Alterations of iron pools have been implicated in diverse human disease processes, including neurodegenerative diseases (*4*, *5*), aging (*4*), microbial infections, atherosclerosis, and cancer (*6*). In order to acquire iron from the environment, cells must solubilize insoluble ferric iron (*7*), transport the iron across a membrane into the cytosol, and regulate the uptake process to maintain cellular iron concentrations within a tightly controlled range. The molecular details of iron transport in most eukaryotes have remained unsolved (*8*, *9*).

High-affinity iron uptake in the yeast *Saccharomyces cerevisiae* requires copper (*10*, *11*). This copper requirement is explained by the involvement of a copper-containing oxidase, FET3, in iron uptake (*10*, *11*). Because the FET3 oxidase activity is required for iron uptake, copper deficiency or mutations in genes involved in delivery of copper to FET3 abrogate iron uptake as a secondary effect. These genes include *CTR1*, the cellular copper uptake transporter (*10*), and *CCC2*, an intracellular copper transporter (*12*). The human multicopper oxidase ceruloplasmin exhibits similarity to the yeast FET3 oxidase (*11*). Ceruloplasmin plays an important role in human iron homeostasis. Copper deficiency has been associated with apparent iron deficiency because of a lack of ceruloplasmin activity (*13*). The inherited disorder, Wilson disease, also associated with deficient ceruloplasmin activity, results from mutations in the gene for a copper-transporting P-type adenosine triphosphatase (ATPase) (*14*) with strong similarity to the CCC2 gene product in yeast (*15*). Severely affected individuals with Wilson disease may exhibit abnormalities of iron transport (*16*). Recently, mutations in the ceruloplasmin gene itself have been identified as the cause of a neurodegenerative syndrome characterized by the failure to export iron from various tissues, including the basal ganglia in the brain (*5*). One interpretation of these findings is that multicopper oxidases (FET3 in yeast, or ceruloplasmin in humans) are required for iron transport across membranes (*17*), although the precise role of such oxidases in mediating iron transport remains unclear. FET3 has a single hydrophobic domain and is localized to the plasma membrane (*18*). Its protein sequence bears no resemblance to that of the family of permeases, and thus it has been difficult to understand how FET3 by itself could mediate iron transport.

We describe another component of the iron uptake system in yeast that fulfills expectations for an iron transporter in having multiple predicted transmembrane domains and iron-binding motifs. Expression is homeostatically regulated through the action of the AFT1 regulatory protein (*19*), as predicted for an element of the iron uptake system and similar to the regulation of FET3 (*11*, *19*). This component appears to work in concert with the FET3 multicopper oxidase to mediate the transmembrane transport of iron into the cell.

FTR1, a candidate gene for the iron transporter. A method for selecting mutants in iron uptake (*10*) or iron sensing (*19*) was devised with the iron-regulated promoter of the *FRE1* gene. Transcription of the *FRE1* gene is repressed in cells grown in the presence of iron (*20*). The *FRE1* promoter was fused to the coding region of the *HIS3* gene and integrated into a haploid yeast strain carrying a deletion at the *HIS3* locus. In this engineered strain, expression of the *HIS3* gene product driven by the *FRE1* promoter was repressed by addition of iron to the growth medium. Spontaneous mutants appeared and grew into colonies on media with high iron and no histidine. Strain E31 (*21*, *22*), which grew under the selective conditions, completely lacked high-affinity iron uptake and was analyzed further. When mutant haploid strains derived from E31 were crossed with strains mutated at the *CTR1*, *CCC2*, or *FET3* loci, the diploids generated by these crosses exhibited normal levels of iron uptake. Thus, E31 contained a recessive mutation in a previously uncharacterized gene required for iron uptake, which we called *FTR1* (for Fe transporter) (*22*).

Evaluation of *FTR1* mutants revealed phenotypic similarity to *FET3* mutants. High-affinity iron uptake was absent (Fig. 1), and manipulation of the copper concentration of the growth medium did not correct this deficiency, even when copper was added at concentrations capable of correcting the defect in a CCC2 mutant (Fig. 1). Growth and colony formation were unimpaired in rich medium or defined medium with sufficient iron (*23*). However, under conditions of iron deprivation created by the iron chelator ferrozine (*24*), growth of the *ftr1-1* mutant and the *fet3-2C* mutant were similarly inhibited (*23*).

To isolate the *FTR1* gene, we trans-

Cell Biology and Metabolism Branch, National Institutes of Child Health and Human Development, National Institutes of Health, Bethesda, MD 20892, USA.

*To whom correspondence should be addressed.

formed the *ftr1-1* mutant strain with a library of wild-type genomic DNA carried on a *URA3* -marked vector (*25*), and the transformants were selected both for uracil prototrophy and the ability to grow on ferrozine-containing plates. One transformant was isolated on the low-iron plates, and the plasmid was recovered from this strain (*26*) (Fig. 2A). An open reading frame (ORF) within the plasmid insert was shown to be required for complementing activity (*26*) (Fig. 2A). The identification of the complementing genomic fragment as the wild-type copy (*FTR1*) of the mutant allele (*ftr1-1*) was further supported by the lack of meiotic recombination between a marked allele of the wild-type genomic clone and the mutant *ftr1-1* allele (*27*). The FTR1 predicted protein hydrophobicity profile was consistent with that of a membrane protein with an NH_2-terminal leader sequence and six predicted transmembrane domains (Fig. 2, B and C) (*28*). Comparison of the amino acid sequence with the protein data base revealed the existence of a homologous gene on chromosome II of *S. cerevisiae*, described as a permease of unknown function in the GenBank annotation. This gene has been named *FTH1*, for FTR1 homolog (*28*). Homologous ORFs were also identified from the distantly related fission yeast *Schizosaccharomyces pombe* and from the bacterium *Bacillus subtilis* (*28*). The *S. pombe* gene showed strong similarity with *FTR1* (45% identity) (*28*) and was transcribed divergently from an ORF with strong similarity to *FET3* (40% identity) (*28*). The *B. subtilis* ORF was shown to contain a consensus binding site for the bacterial iron-regulatory protein Fur (*29*) within its 5′ flanking sequences (*28*). When the amino acid sequences for the FTR1 homologs were aligned, a conserved five–amino acid motif, REG(L/M)E (*28*, *30*), was observed embedded in a hydrophobic region (Fig. 2D). Mammalian ferritin light chains contain a similar amino acid motif, REGAE (*30*), in which the glutamic acid residues interact directly with iron (*31*).

The *FTR1* transcript was examined by probing total RNA with a labeled DNA fragment derived from the predicted ORF. The observed transcript size (1.7 kb) was sufficiently large to encode the predicted protein. Expression of *FTR1* mRNA was induced by iron starvation and was *AFT1*-dependent. *AFT1* encodes an iron-regulated transciptional activator (*19*, *32*). Thus, *FTR1*, like *FET3*, can be considered to form part of an iron-controlled regulon. This regulated character of the *FTR1* gene fulfills a key prediction for a component of the iron uptake system.

The similar phenotypes of loss-of-function mutations of *FET3* or *FTR1* suggested that the two proteins might interact, either directly or indirectly. We tested this possibility by using high–copy number plasmids to vary the expression of the two proteins independently (*33*). Expression of *FET3* alone from a multicopy plasmid, which increased FET3 protein expression (*34*), did not result in increased iron uptake (Fig. 3), nor did expression of *FTR1* alone. Only when *FTR1* and *FET3* were simultaneously overexpressed on multicopy plasmids was iron uptake increased above that of the wild

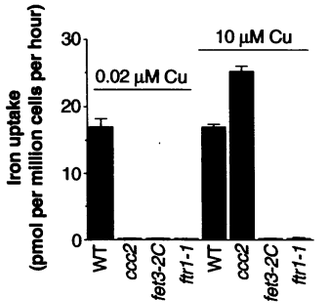

Fig. 1. Similarity of *ftr1-1* and *fet3-2C* mutant strains. Failure of copper to correct iron uptake deficiency of the *ftr1-1* and *fet3-2C* mutants. The parental strain 61 (WT) and mutant strains YRS3 (*ccc2*), 2C (*fet3-2C*), and TR1 (*ftr1-1*) (*21*) were grown in modified SD medium lacking iron and with copper added as indicated. High-affinity iron uptake was measured as described (*10*). Uptake data are means (±SD) of three replicates.

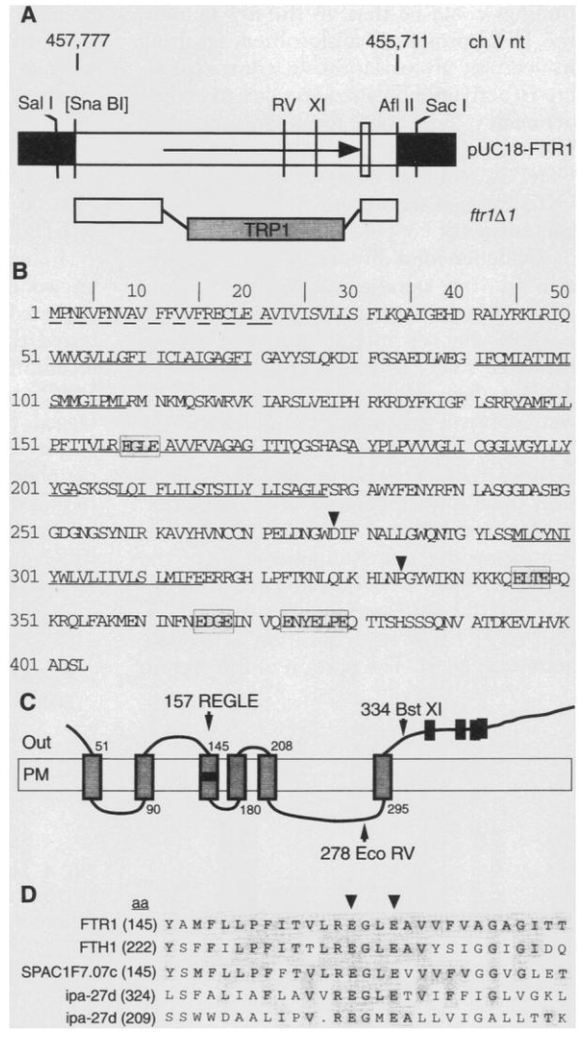

Fig. 2. *FTR1* gene and predicted protein. (**A**) (Top) The genomic fragment capable of complementing the iron uptake defect in the *ftr1-1* strain is shown (▭) with the chromosome V location (ch V nt). Genomic restriction sites Afl II, XI (Bst XI), RV (Eco RV), and [Sna BI] are shown. The brackets around Sna BI indicate that this site was destroyed during a blunt-end cloning step. The pUC18 vector sequences (▬) are shown with the unique cloning sites Sal I and Sac I. The FTR1 ORF (identical with YER145c, chromosome V nt 457,249 to 456,035) is indicated by an arrow (→) (*26*). Also shown is the insertion site for the MYC epitope at the COOH-terminus of the FTR1 predicted protein (□) (*37*). (Bottom) Map of the *ftr1Δ1* allele (*35*). (**B**) FTR1 protein predicted amino acid sequence: Conceptual translation of the *FTR1* ORF (*30*). A probable leader sequence is indicated by a dashed line, and six predicted transmembrane domains are shown underlined (*28*). Downward arrowheads indicate the amino acid residue immediately preceding the stop codons in the Bst XI and Eco RV truncations (*26*). All occurrences of the amino acid motif EXXE are boxed. (**C**) FTR1 protein topology. The plasma membrane (PM) is shown as a shaded rectangle. The FTR1 protein is shown as a black ribbon with six cylinders representing the predicted transmembrane domains (numbers are FTR1 protein amino acid numbers referring to the first amino acid of each transmembrane domain). Dark boxes indicate EXXE motifs. The REGLE motif and the locations of the Eco RV and Bst XI truncations are indicated by arrows (numbers refer to the first amino acid of the motif and the last amino acids included in the truncated proteins, respectively). (**D**) FTR1 protein homologs. FTR1 (*S. cerevisiae*), FTH1 (*S. cerevisiae*), SPAC1F7.07c (*S. pombe*), ipa-27d (*B. subtilis*) predicted amino acid sequences were aligned around the REG(L/M)E motifs (*28*). The hydrophobic domains surrounding these motifs are shown. The amino acid number at the beginning of the aligned region is shown next to the ORF name. Shaded letters represent residues identical with the FTR1 protein sequence. Downward arrowheads point to the conserved E residues in the FTR1 protein, shown by mutagenesis to be required for iron transport.

type (Fig. 3). Thus, both genes encode limiting components of the iron uptake system.

The *ftr1* mutant strains were then examined for FET3 oxidase activity. Surprisingly, the *ftr1-1* allele was associated with markedly diminished FET3 oxidase activity (Fig. 4), whereas the *ftr1* null allele (*35*) resulted in unmeasurable levels of activity. Because the FET3 oxidase activity could be restored in vitro by addition of copper to the lysate (Fig. 4), the defect appeared to be a consequence of failure to insert copper into the FET3 protein. This copper-reconstituted FET3 oxidase activity migrated aberrantly on a gel (Fig. 4). However, after treatment of the extracts with endoglycosidase H, the mobility of the copper-reconstituted oxidase was indistinguishable from that of the control (Fig. 4). An explanation for these findings could be that, in the *ftr1* mutant, the FET3 protein is mislocalized, resulting in aberrant glycosylation. In contrast, failure to activate FET3 oxidase due to copper deficiency does not result in abnormal FET3 glycosylation (*12*), suggesting that *FTR1* is required both for maturation of FET3 through the secretory pathway and its acquisition of copper.

Evidence for a direct role of FTR1 protein in iron uptake. Because *FTR1* was required for oxidase activity (Fig. 4), it was possible that its role in iron uptake was mediated solely by its effects on the FET3 oxidase. Several mutant alleles of *FTR1* were constructed in order to dissociate the role of *FTR1* in promoting FET3 oxidase activity from a possible independent role in iron uptake. Introduction of a translation termination codon at the unique Bst XI site, truncating the last 70 amino acids of the predicted protein (*26*), abrogated iron uptake but did not interfere with the maturation of FET3 or its acquisition of oxidase activity (Fig. 5). The portion of the protein removed by this truncation included numerous acidic residues and four repeats of the degenerate consensus sequence EXXE (Fig. 2). Removal of an additional 54 amino acids by introduction of a stop codon at an upstream Eco RV site abolished both oxidase activity (FET3 protein maturation) and iron uptake (Fig. 5). The REGLE motif was then mutated by site-directed mutagenesis. Each glutamate residue of the motif was changed to an alanine, individually or together (36). The mutated *FTR1* constructs were then introduced into an *ftr1* null strain, and the transformants were evaluated for iron uptake and oxidase activity. In each of the REGLE mutants, iron uptake was virtually absent, whereas FET3 oxidase activity was unaffected (Fig. 5). Thus, the FTR1 protein was bifunctional: Some portions of the protein were required for oxidase activity of the FET3 protein, whereas other portions were required for mediation of iron uptake. The *FTR1* allele–specific effects on the FET3 oxidase indicated an association between these two gene products. The *FTR1* allele–specific effects on iron uptake suggested a direct role of FTR1 protein in iron transport.

In order to mediate iron uptake from the environment, the FTR1 protein would be expected to reside on the cell surface. We tested this hypothesis by determining the localization of the FTR1 protein, using a MYC epitope–tagged protein (*37*, *38*). The tagged protein could be visualized as a bright rim of immunofluorescence at the periphery of the cell, consistent with localization to the plasma membrane (Fig. 6). In contrast, in a *fet3* deletion strain, the tagged FTR1 protein was not apparent on the cell surface. It was present instead in perinuclear ringed structures, consistent with localization to the endoplasmic reticulum (ER) (Fig. 6, C and D). When *FET3* was retransformed into this strain on a plasmid, the distribution of the FTR1 protein shifted to the cell surface, and the internal structures were no longer apparent (Fig. 6A). The REGLA point mutant was evaluated in a similar manner. Its localization was indistinguishable from that of the wild-type FTR1 protein, appearing on the plasma membrane when the *FET3* gene was present (Fig. 6B).

An iron transport complex. A scheme that accounts for our findings is shown in Fig. 7. FET3 and FTR1 proteins assemble into a complex in a cellular compartment early in the secretory pathway, most likely in the ER. The complex progresses to a post-Golgi compartment (*39*), where the CCC2 protein mediates copper delivery to FET3. Finally, the copper-loaded FET3 protein, presumably still complexed to FTR1 protein, is delivered to the plasma membrane and becomes competent for iron transport. The point mutation in FTR1, altering a single glutamic acid residue of the REGLE motif, interferes only with iron transport, thereby specifically implicating the FTR1 protein in the transport process.

The requirement of external ferric re-

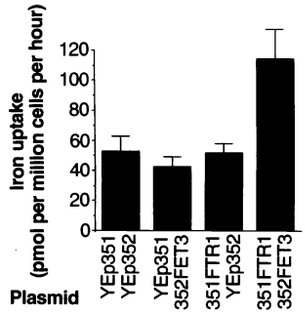

Fig. 3. Both *FET3* and *FTR1* are limiting for iron uptake. The wild-type strain YPH250 (*21*) was transformed with the following high copy number plasmids: (i) YEp351 and YEp352, (ii) YEp351 and 352FET3, (iii) 351FTR1 and YEp352, and (iv) 351FTR1 and 352FET3 (*26*). The transformants were grown in iron-free medium before measurement of iron uptake activity (six replicates). Uptake data are means (±SD).

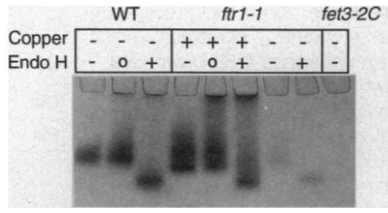

Fig. 4. Mutant *ftr1* allele associated with lack of FET3 oxidase. An activity gel is shown in which the activity of the FET3 oxidase was visualized as precipitant bands of *p*-phenylenediamine substrate. Strains CM3260 (WT), TR1 (*ftr1-1*), and 2C (*fet3-2C*) (*21*) were grown in YPD medium. Cells were harvested and lysed in buffer (*12*) lacking copper (−) or with 50 μM added copper sulfate (+). Some samples were treated with 1000 U of endoglycosidase H (New England Biolabs) for 4 hours at 37°C in lysis buffer (+), whereas other samples were incubated in buffer alone under identical conditions (o). Twenty micrograms of solubilized membrane protein from each sample were separated by SDS–polyacrylamide gel electrophoresis, and oxidase activity was visualized as described (*12*).

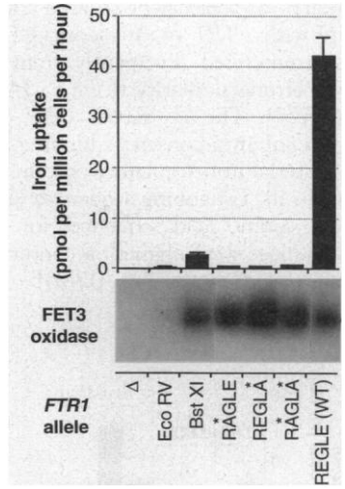

Fig. 5. Effects of *FTR1* mutations on FET3 oxidase and iron uptake. Strain 42C (*ftr1Δ1*) (*21*, *35*) was transformed with plasmid YEp351 (Δ) or with the same plasmid containing mutant alleles of *FTR1*. The mutant alleles included truncations of the COOH-terminal domain at the Eco RV site (Eco RV) or the Bst XI site (Bst XI) and point mutants (*) altering the first glutamic acid residue of the REGLE motif (RAGLE), the second glutamic acid of the motif (REGLA), or both together (RAGLA). The unmodified genomic fragment in YEp351 was also included as a control [REGLE (WT)] (*36*). These transformants were grown in iron-free medium and assayed for iron uptake and oxidase activity. Uptake data are the means of triplicate determinations (±SD).

ductases for ferric iron uptake (*20*, *40*) suggests that ferrous iron is the substrate for transmembrane transport. What is then surprising is that iron transport requires an active oxidase outside of the cell. To understand how this oxidase functions in mediating iron transport will require identification of its substrate. Perhaps ferrous iron is also the substrate for the oxidase. One could speculate that the FTR1 protein contains binding sites for both ferrous and ferric iron, with ferrous iron representing the intially bound species. Subsequent oxidation of the bound ferrous iron might result in transfer to a ferric iron binding site and perhaps in a conformational change in the transporter, processes that could be coupled to transmembrane transport.

Insight into the process of iron transport may be obtained from studies of ferritin. Ferritin is a protein found in the cytoplasm of vertebrate cells, where it assembles into a 24-subunit, hollow spherical complex capable of taking up and storing iron (*31*). The subunits are a mixture of heavy chain ferritin, which has ferroxidase activity, and light chain ferritin, which lacks enzymatic activity. Data from crystal structures and site-directed mutagenesis indicate that a hydrophilic "spine" consisting of carboxylate residues leads from the exterior of the ferritin shell to the iron nucleation site in the interior (*31*). Glutamic acid residues of a motif present in light chains, REGAE (horse sequence), are thought to participate in the nucleation site for iron core formation (*31*). Thus, the iron-interacting carboxylate residues in ferritin may play a role analogous to that played by the glutamates in the REGLE motif of the FTR1 permease, which are essential for iron transport. In contrast to the ferritin sequence motifs, however, the critical motif of the FTR1 protein is situated within a hydrophobic domain (Fig. 2D), consistent with a role in transport of iron through a membrane.

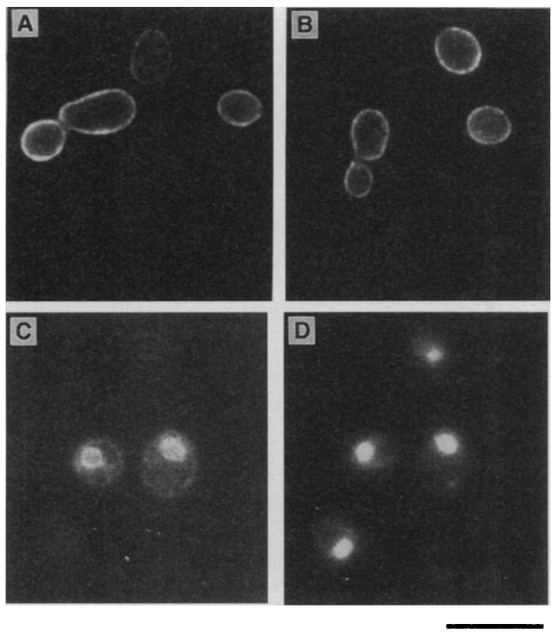

Fig. 6. Influence of *FET3* on localization of FTR1 protein visualized by immunofluorescence (*49*). Strain YPHfa (Δ*fet3*) (*21*) was transformed with the following constructs: (**A**) 702FTR1myc (contains the *FTR1* gene with a COOH-terminal MYC epitope) (*37*) and 352FET3 (contains *FET3*) (*26*); (**B**) 702REGLAmyc (contains a mutated form of FTR1 with MYC tag) (*36*) and 352FET3; (**C** and **D**) 702FTR1myc and YEp352. The transformants were grown in iron-depleted medium, fixed, and stained with antibodies to the MYC epitope (A to C) or with DAPI (D). Bar, 10 μm.

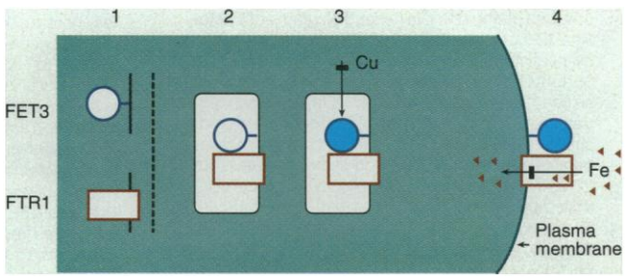

Fig. 7. Model for assembly of an iron-transport complex. The shaded area depicts the interior of a cell with the plasma membrane to the right. (Step 1) Biosynthesis of FTR1 (brown rectangle) and FET3 (blue circle with a line representing its membrane attachment). Deletion of the genes for FET3 or FTR1 results in retention of the other component in this internal compartment, probably the ER (block indicated by a dashed line). (Step 2) Assembly of the two components in the membrane of the ER. (Step 3) Copper-loading of FET3 protein in a post-Golgi compartment (*39*) and mediated by CCC2. Mutations at the *CCC2* locus result in synthesis of inactive FET3 apoprotein because of failure to transport copper into this compartment (block indicated by a black rectangle). (Step 4) Appearance of the FET3-FTR1 complex on the plasma membrane, where the complex mediates iron uptake into the cell. A point mutation in the REGLE motif of the FTR1 protein specifically interferes with iron transport (depicted by the black rectangle within FTR1).

Generality of the yeast model. We have proposed that a multicopper oxidase, FET3, and a permease, FTR1, comprise a molecular complex responsible for translocating iron from the environment into the cell. What is the generality of this model for iron transport? Examination of the protein data base suggests that homologs for both *FET3* (*41*) and *FTR1* (*28*) exist in *S. cerevisiae*. These might function to transport iron out of the cell or across some other organelle membrane, such as the vacuole, ER, Golgi, or mitochondria. In the distantly related yeast *S. pombe*, an iron-regulated surface ferric reductase (*42*) and homologs of both *FET3* (*28*) and *FTR1* (*28*) have been identified. Furthermore, the *FET3* and *FTR1* homologs lie adjacent to one another in the genome and are transcribed divergently, suggesting coordinate regulation. In bacteria, a *B. subtilis* homolog of *FTR1* has been identified (*28*) that might function to transport iron after its release from a siderophore, or as part of an alternative uptake system.

Several lines of evidence indicate that the copper-dependent iron transport characterized in *S. cerevisiae* is likely to be relevant to iron transport in humans. Copper deficiency results in secondary iron deficiency as a consequence of failure to provide cofactor to ceruloplasmin, a copper protein with an oxidase activity similar to that of FET3 (*11*). The P-type ATPase encoded by the Wilson disease gene is required to deliver copper to ceruloplasmin (*14*), analogous to the requirement for CCC2 (*15*) in the delivery of copper to FET3 in yeast (*12*). Recently, mutations in the gene for human ceruloplasmin have been identified that result in a neurologic syndrome attributed to the failure to appropriately transport iron into or out of the basal ganglia (*5*). Other neurodegenerative diseases have also been linked to iron deposition in neural tissues, including Hallervorden-Spatz syndrome, Parkinson's disease, and Alzheimer's disease (*4*). These observations suggest that the coupling between a copper-dependent oxidase and an iron permease represents an evolutionarily conserved mechanism of iron transport in eukaryotes, and that perturbations in such mechanisms may be a contributing factor in certain neurodegenerative diseases.

REFERENCES AND NOTES

1. R. Cammack, J. M. Wrigglesworth, H. Baum, in *Iron Transport and Storage*, P. Ponka, H. M. Schulman, R. C. Woodworth, Eds. (CRC Press, Cleveland, OH, 1990), pp. 17–39.
2. K. Karlin, *Science* **261**, 701 (1993).
3. B. Halliwell and J. M. C. Gutteridge, *Free Radicals in Biology and Medicine* (Clarendon, Oxford, UK, 1991).
4. On the relation of iron to aging and degenerative

neurologic diseases: X. Wang, F. Manganaro, H. M. Schipper, *J. Neurochem.* **74**, 1868 (1995); M. Gerlack, D. Benshachar, P. Riederer, M. B. Youdim, *ibid.* **63**, 793 (1994). Hallervorden-Spatz syndrome: E. C. Dooling, E. P. Richardson Jr., K. R. Davis, *Neurology* **30**, 1128 (1980); E. C. Dooling, W. C. Schoene, E. P. Richardson Jr., *Arch. Neurol.* **30**, 70 (1974). Parkinson's disease: J. M. Gorell *et al.*, *Neurology* **45**, 1138 (1995).

5. Aceruloplasminemia: Z. L. Harris *et al.*, *Proc. Natl. Acad. Sci. U.S.A.* **92**, 2539 (1995); K. Yoshida *et al.*, *Nat. Genet.* **9**, 267 (1995); H. Miyajima *et al.*, *Neurology* **37**, 761 (1987).
6. On the relation of iron to microbial infections: E. D. Weinberg, *J. Pharmacol.* **16**, 358 (1985). Atherosclerosis: C. Smith, M. J. Mitchinson, O. I. Aruoma, B. Halliwell, *Biochem. J.* **286**, 901 (1992); J. T. Salonen *et al.*, *Circulation* **86**, 803 (1992). Hemochromatosis and hepatoma: A. Bomford and R. Williams, *Q. J. Med.* **45**, 611 (1976).
7. R. J. P. Williams, in (*1*), pp. 2–15.
8. The transport of iron characterized here must be distinguished from the transport of iron-siderophore complexes that occurs in most bacteria. Bacteria secrete high-affinity ferric iron chelators called siderophores (*43*), and iron transport is achieved by uptake of the ferrisiderophore complex (*43*). Most eukaryotes, including *S. cerevisiae*, do not synthesize siderophores (*44*).
9. Genetic studies in *E. coli* have led to identification of the *feo* gene as a candidate iron transporter, functioning in the absence of siderophores under anaerobic growth conditions [M. Kammler, C. Schon, K. Hantke, *J. Bacteriol.* **175**, 6212 (1993)]. In *S. cerevisiae*, iron uptake requires the sequential action of externally directed ferric reductases (encoded by the *FRE1* and *FRE2* genes), and a high-affinity ferrous iron transport system (subject of this paper) or a low-affinity ferrous transport system encoded by *FET4* [D. R. Dix, J. T. Bridgham, M. A. Broderius, C. A. Byersdorfer, D. Eide, *J. Biol. Chem.* **269**, 26092 (1994)]. Homologs of *FET4* or *feo* have not been identified in other species. In humans, candidate iron transporters have been identified through isolation of iron-binding proteins from human intestine [M. E. Conrad *et al.*, *Blood* **81**, 517 (1993)] and through in vitro studies of the proton-pumping ATPase of erythrocytes [C. Li, J. A. Watkins, J. Glass, *J. Biol. Chem.* **269**, 10242 (1994)]. For a review of human iron metabolism, see G. M. Brittenham, in *Hematology, Basic Principles and Practice*, R. Hoffman *et al.*, Eds. (Churchill Livingstone, New York, 1995), pp. 492–523. The human genetic disease hemochromatosis, characterized by unregulated iron accumulation and consequent organ damage, has been described by T. H. Bothwell, R. W. Charlton, and A. G. Motulsky [in *The Metabolic and Molecular Bases of Inherited Disease*, C. R. Scriver, A. L. Beaudet, W. S. Sly, D. Valle, Eds. (McGraw-Hill, New York, 1995), pp. 2237–2269]. The gene for this disease has not been cloned.
10. A. Dancis *et al.*, *Cell* **76**, 393 (1994).
11. C. Askwith *et al.*, *ibid.*, p. 403.
12. D. S. Yuan *et al.*, *Proc. Natl. Acad. Sci. U.S.A.* **92**, 2632 (1995).
13. G. R. Lee, S. Nacht, J. N. Lukens, G. E. Cartwright, *J. Clin. Invest.* **47**, 2058 (1968).
14. P. C. Bull *et al.*, *Nat. Genet.* **5**, 327 (1993); R. E. Tanzi *et al.*, *Ibid.*, p. 344; Y. Yamaguchi, M. E. Heiny, J. D. Gitlin, *Biochem. Biophys. Res. Commun.* **197**, 271 (1993).
15. D. Fu, T. J. Beeler, T. M. Dunn, *Yeast* **11**, 283 (1995).
16. H. P. Roeser, G. R. Lee, S. Nacht, G. E. Cartwright, *J. Clin. Invest.* **49**, 2408 (1970); S. O'Reilly, M. Pollycove, W. J. Bank, *Neurology* **18**, 634 (1968).
17. S. Osaki, D. A. Johnson, E. Frieden, *J. Biol. Chem.* **241**, 2746 (1966).
18. D. M. De Silva, C. Askwith, D. Eide, J. Kaplan, *ibid.* **270**, 1098 (1995).
19. Y. Yamaguchi-Iwai, A. Dancis, R. D. Klausner, *EMBO J.* **14**, 1231 (1995).
20. A. Dancis, D. G. Roman, G. J. Anderson, A. G. Hinnebusch, R. D. Klausner, *Proc. Natl. Acad. Sci. U.S.A.* **89**, 3869 (1992).
21. Yeast strains: Strain CM3260 was modified by integration of the FRE1-HIS3 fusion to create strain 61 (*10*). Strains derived from 61 (*MATα gcn4-101 his3-609 leu2-3,112 trp1-63 ura3-52 FRE1-HIS3::URA3*): E30 (*ma15-2, fet3-2C*); E10 (*ma15-3 ftr1-1*); E31 (*ma15-4 ftr1-2*); TR1 (*ftr1-1*); 64 (*Δctr1::LEU2*); YRS3 (*ccc2::URA3*). M2 (*AFT1-1^{up}*) (*19*), Y18 (*aft1::TRP1*) (*19*). Strains derived from the related strain 81 (*MATa gcn4-101 his3-609 leu2-3,112 ino1-13 ura3-52 FRE1-HIS3::URA3*): TR4 (*ftr1-2*); 2C (*fet3-2C*). Mutations at the *MA15* locus, for which the gene has not been cloned, result in high iron uptake. TR1p was created by patching TR1 onto 5-fluoroorotic acid plates to eject the *FRE1-HIS3* construct and recover the uracil auxotrophy. DEY1397-6A (*MATα ura3-52 leu2-3,112 trp1-1 his3-11,15 ade2-1 can1-100 fet3::HIS3*) (*11*) was used in several crosses. Strains with a different genetic background were derived from the parental strain YPH252 (*MATα ura3-52 lys2-801 ade2-101 trp1-Δ1 his3-Δ200 leu2-Δ1*): YPHfa (*Δfet3::TRP1*) (*12*). The parental strain of the opposite mating type, YPH250, was used to construct a deletion of *FTR1*, strain 42C (*ftr1Δ1::TRP1*).
22. Mutant selection: Strain 61 was grown on agar plates made from modified SD medium lacking histidine and including 100 μM ferric ammonium sulfate, 10 μM copper sulfate, and 50 mM MES buffer (pH 6.1). Strains E10 (*ma15-3 ftr1-1*), E31 (*ma15-4 ftr1-2*), and E30 (*ma15-2 fet3-2C*) were derived from colonies that appeared on these plates after 8 days. They were evaluated and found to be deficient in iron uptake. Diploids formed by crossing these strains with strain 81 exhibited normal iron uptake activity. The E10x81diploid was then sporulated, and spore clones were sorted into three categories: (i) Single mutants lacking iron uptake (*ftr1-1*); (ii) single mutants with high iron uptake (*ma15-3*); and (iii) double mutants lacking iron uptake (*ma15-3 ftr1-1*). The double mutants could be identified, because backcrossing to the parental strains 81 or 61 and sporulation resulted in segregation of the high iron uptake and low iron uptake traits in the spore clones. Strain TR1 (*ftr1-1*) was derived from a spore clone lacking iron uptake activity and with a single mutation. In a similar manner, the E31x81 diploid was sporulated, and spore clone TR4 (*ftr1-2*) was identified. The diploid strain, E30x81, was sporulated, and spore clone 2C (*fet3-2C*) was identified. 2C (*fet3-2C*) was found to contain a mutant allele of *FET3*, because a diploid formed by crossing with DEY1397-6A (*fet3::HIS3*) lacked iron uptake activity. TR1 (*ftr1-1*) and TR4 (*ftr1-2*) were found to contain mutant alleles of the same gene, because the diploid formed by crossing TR1 with TR4 lacked iron uptake activity. Mating of TR4 with strains 64 (*Δctr1::LEU2*), DEY1397-6A (*fet3::HIS3*), or YRS3 (*ccc2::URA3*) yielded diploids, each with normal iron uptake activity.
23. Strains 61 (parental), 2C (*fet3-2C*), and TR1 (*ftr1-1*) were spread onto agar plates containing YPD (2% yeast extract, 1% peptone, and 2% glucose), or SD modified to contain sufficient iron or limited iron. Formulation of the modifed SD plates (per liter): 6.7 g yeast nitrogen base without amino acids (Difco), 0.8 g CSM or CSM-ura (Bio101), 20 g glucose, 50 mM MES (pH 6.1) (Sigma), and 1 mM ferrozine (Fluka). The ingredients were dissolved in distilled, deionized water and filter-sterilized through a 0.45-μm nitrocellulose membrane (Nalgene). Ten grams of Bacto-Agar (Difco) were added to the filtrate and dissolved by heating in a microwave oven. After cooling to 55°C, a freshly dissolved stock of ferrous ammonium sulfate (10 mM, Fluka) was added to a final concentration of 50 μM (iron-limited plates) or 350 μM (iron-sufficient plates). All strains formed colonies of comparable size on the YPD or iron-sufficient plates, but 2C and TR1 formed only micro-colonies on the iron-limited plates.
24. R. L. Chaney, *J. Plant Nutr.* **11**, 1033 (1988); L. L. Stookey, *Anal. Chem.* **42**, 779 (1970).
25. M. D. Rose, P. Novick, J. H. Thomas, D. Botstein, G. R. Fink, *Gene* **60**, 237 (1987).
26. Cloning of *FTR1* and identification of the complementing ORF: TR1p was transformed with a yeast genomic library, and plamid YCp50/FTR1.1 was recovered from the transformed Ura$^+$ colony growing on low-iron plates. Using primers flanking the Bam HI site, we sequenced the ends of the yeast DNA insert, and the complementing region was narrowed to the Sna BI–Afl II fragment of 2065 base pairs (bp) [chromosome V, nt 457,777 to 455,711] containing the ORF YER145c (GenBank accession number U18917). This fragment was subcloned into pUC18 for further manipulations (pUC18/FTR1). Identification of the *FTR1* ORF: pUC18/FTR1 was digested with either Eco RV or Bst XI. The Bst XI 3′ overhang was removed with T4 DNA polymerase, and an oligonucleotide was ligated to the blunt ends, introducing stop codons in three frames at the Eco RV or Bst XI sites of the *FTR1* ORF. The *FTR1* constructs in pUC18 were then returned to yeast shuttle vectors, creating the following plasmids: 351FTR1 (genomic fragment in high copy number vector with LEU2 marker), 351FTR1tBstXI (same, but with *FTR1* coding region truncated at Bst XI site), and 351FTR1tEcoRV (same, but with *FTR1* coding region truncated at Eco RV site). The truncated variants of the *FTR1* ORF were unable to complement the iron uptake defect of TR1p (*ftr1-1*). *FET3* plasmid: A 2.8-kb Hind III–Eco RV genomic fragment derived from the clone pDS8 (*11*) was inserted in plasmid YEp352, creating plasmid 352FET3 (high copy number with *URA3* marker).
27. The marked strain 42C(*ftr1Δ1::TRP1*) was crossed with TR1(*ftr1-1*) and sporulated. Tetrads from 24 meioses were evaluated, and all segregants were deficient in iron uptake.
28. The conceptual translation of the *FTR1* ORF was analyzed with the TMpred program (*45*). This same amino acid sequence was then used to query the sequence data base (non-redundant PDB + GBupdate + GenBank + EMBLupdate + EMBL, 14 November 1995) with the BLAST algorithm (*46*). Similar ORFs identified were as follows: YBR207w (GenBank accession number Z36076) from chromosome II of *S. cerevisiae*, which we have called FTH1, gave a probability score of 4.0e-84. SPACIF7.07c (accession number Z67998) from *S. pombe* gave a probability score of 2.2e-105. An adjacent and divergently transcribed ORF in *S. pombe*, SPAC1F7.08 (accession number Z67998), was similar to FET3 and gave a probability score of 2.0e-120. ipa-27d (accession number X73124) of *B. subtilis* gave a probability score of 6.4e-07 when compared with FTR1. The PileUp program (*47*) was used to align similar amino acid sequences, and BESTFIT (*47*) was used to determine percent identity between similar proteins.
29. A. Bagg and J. B. Nielands, *Biochemistry* **26**, 5471 (1987).
30. Single-letter abbreviations for the amino acid residues are as follows: A, Ala; C, Cys; D, Asp; E, Glu; F, Phe; G, Gly; H, His; I, Ile; K, Lys; L, Leu; M, Met; N, Asn; P, Pro; Q, Gln; R, Arg; S, Ser; T, Thr; V, Val; W, Trp; and Y, Tyr.
31. Prosite entries PS00540, PS00204 for ferritin metal binding sites; R. R. Crichton, in *Inorganic Biochemistry of Iron Metabolism* (Horwood, New York, 1991), pp. 144–154; S. Levi *et al.*, *J. Mol. Biol.* **238**, 649 (1994); S. J. Lippard and J. M. Berg, *Principles of Bioinorganic Chemistry* (University Science Books, Mill Valley, CA, 1994), pp. 125–130; J. Trikha, E. C. Theil, N. M. Allewell, *J. Mol. Biol.* **248**, 949 (1995).
32. RNA blot analysis was used to examine *FTR1* transcripts from 61 (parent), M2 (*AFT1-1^{up}*), and Y18 (*aft1* interruption) strains (*21*), each grown in iron-replete or iron-starved media. The *FTR1* mRNA was induced by iron deprivation and repressed by iron availability in strain 61, but was constitutively present in the M2 strain and virtually undetectable in the Y18 strain (Y. Yamaguchi-Iwai, R. Stearman, A. Dancis, R. D. Klausner, in preparation).
33. J. Rine, *Methods. Enzymol.* **194**, 239 (1991).
34. Rabbit antibody against FET3 protein (*39*) was used to evaluate FET3 protein levels by immunoblotting of cell lysates from the wild-type strain YPH252 and the same strain transformed with plasmid 352FET3. The protein was overexpressed roughly fivefold in the transformed strain.
35. Deletion of FTR1 from the genome: For constructing strain 42C (*ftr1Δ1::TRP1*), 200-bp DNA fragments flanking the *FTR1* ORF were generated by PCR. The 5′ fragment contained a unique Acc65 I site, and the 3′ fragment contained a Bgl II site adjacent to the coding region. A third fragment containing the *TRP1* gene was generated by PCR with matching restriction sites. These fragments were digested and ligat-

ed in vitro, and then PCR with flanking primers was used to amplify the entire construct. The PCR-generated fragment was used to transform YPH250 to prototrophy for tryptophan, and the correctness of the genomic insertion was validated by PCR from the *TRP1* marker and flanking DNA sequences in the genome.
36. Mutagenesis of FTR1: Point mutations were introduced into the plasmid 351FTR1 by standard protocols (Chameleon, Stratagene). The REGLE amino acid sequence motif of the FTR1 protein was mutated to RAGLE, REGLA, or RAGLA, creating plasmids 351RAGLE, 351REGLA, and 351RAGLA. The presence of the expected mutations was verified by sequencing, and three independently derived mutant clones were used in these experiments. The Sst I–Eco RV fragment of plasmid 351REGLA, containing the mutated sequences, was used to replace the corresponding fragment in pUC18-FTR1myc. The entire Sst I–Sal I fragment was then transferred to the corresponding sites of p702, creating 702REGLAmyc.
37. Epitope tag insertion: The 10–amino acid MYC tag sequence (EQKLISEEDL) (*38*) was introduced at the COOH-terminus of the FTR1 protein in two steps. First, the restriction sites, Bgl II and Spe I, were inserted at the COOH-terminus of the *FTR1* ORF in plasmid pUC18-FTR1. This was accomplished by PCR to generate a replacement fragment with the additional restriction sites between the genomic Bst XI and Dra III sites. Two amino acids (lysine and serine) were added to the COOH-terminus of the FTR1 protein as a result of introducing the Bgl II site. Next, complementary, synthetic oligonucleotides encoding the MYC tag flanked by Bgl II and Spe I cohesive ends were synthesized. These oligonucleotides were annealed and ligated into the corresponding restriction sites of the modified pUC18-FTR1 plasmid. The plasmid, pUC18-FTR1myc, was sequenced between the Bst XI and Dra III sites, thereby verifying the presence of the sequences coding for the added COOH-terminal amino acids KSEQKLSEEDL. The *FTR1* constructs in pUC18 were returned to yeast shuttle vectors, creating the plasmids 351FTR1myc (genomic fragment with MYC tag added at the COOH-terminus of the coding sequence) and 702-FTR1myc (same fragment in a low copy number vector with LEU2 marker). The epitope insertion did not interfere with the ability of the modified *FTR1* to complement the iron uptake defect of an *ftr1* deletion strain, 42C (*21*).
38. P. A. Kolodziej and R. Young, *Methods Enzymol.* **194**, 508 (1991).
39. D. S. Yuan, A. Dancis, R. D. Klausner, in preparation.
40. E. Lesuisse, F. Raguzzi, R. R. Crichton, *J. Gen Microbiol.* **133**, 3229 (1987); E. Georgatsou and D. Alexandraki, *Mol. Cell. Biol.* **14**, 3065 (1994).
41. ORF name YFL041w (GenBank accession number P38993).
42. D. G. Roman, A. Dancis, G. J. Anderson, R. D. Klausner, *Mol. Cell. Biol.* **13**, 4342 (1993).
43. J. B. Nielands, *Annu. Rev. Nutr.* **1**, 27 (1981).
44. G. Winkelmann, J. Van Der Helm, J. B. Nielands, Eds., *Iron Transport in Microbes, Plants and Animals* (VCH, Weinheim, Germany, 1987).
45. K. Hofmann and W. Stoffel, *Biol. Chem. Hoppe-Seyler* **347**, 166 (1993)
46. S. F. Altschul, W. Gish, W. Miller, E. W. Myers, D. J. Lipman, *J. Mol. Biol.* **215**, 403 (1990).
47. Program Manual for the Wisconsin Package, Version 8 (Genetics Computer Group, Madison, WI, 1994).
48. C. J. Roberts, C. K. Raymond, C. T. Yamashiro, T. H. Stevens, *Methods Enzymol.* **194**, 644 (1991).
49. Immunofluorescence: Strains were grown in iron-free medium and fixed in formaldehyde. Treatment for 1 hour with oxylyticase (1 mg/ml; Enzogenetics) was followed by a 2-min treatment with 2% SDS. After removal of SDS, the cells were fixed to poly-lysine-coated cover slips (*48*). The cover slips were incubated with 9E10 ascites (1:1000), washed, and incubated with Cy3-conjugated rabbit antibody to mouse immunoglobulin G (Jackson Immunoresearch). In some instances, DAPI (Sigma) was added to stain the nucleus. Cells were visualized with a Zeiss photomicroscope.
50. We thank F. S. Dietrich for providing sequence information from the *S. cerevisiae* genome project before publication; J. Bonifacino, T. Rouault, G. Storz, and J. Stubbe for critical review of the manuscript and helpful conversations and comments; and N. Brun and J. Kelly for assisting with preparation of Fig. 7.

7 December 1995; accepted 5 February 1996